SUPPORTING INFORMATION

Effect of Positional Isomerism in the Excited State Charge Transfer Dynamics in Anthracene-based D-π-A Systems

Swatilekha Pratihar, and Edamana Prasad*

Department of Chemistry, Indian Institute of Technology Madras, Chennai-600036, Tamil Nadu, India.

***Corresponding author email**: pre@iitm.ac.in

Table of Contents

Figure S14. Nanosecond transient absorption spectra and decay trace of *meta*-CN in absence and in presence of DEA in MCH

Figure S15. Semilogarithmic plot of ns transient data of *ortho*-CN and *meta*-CN in presence of DEEA in MCH

Figure S16. Comparative nanosecond transient absorption spectra of *ortho*-CN and DEA/*ortho*-CN at same time delays and 450 nm decay trace of DEA/*ortho*-CN pair in MCH

Figure S17. Comparative nanosecond transient absorption spectra of *meta*-CN and DEA/*meta*-CN at same time delay and 450 nm decay trace of DEA/ *meta*-CN pair in MCH

Figure S18. Comparative nanosecond transient absorption spectra of *ortho*-CN and DPA/*ortho*-CN and decay plot of DPA radical

Figure S19. Comparative nanosecond transient absorption spectra of *meta*-CN and DPA/*meta*-CN and decay plot of DPA radical

Figure S20. TAS spectra and decay trace of reference molecule AnPh isomer in absence and presence of quencher DEA at different delay times

SI-A: Experimental Section

Materials: UV-grade solvents (tetrahyrofuran, methylcyclohexane, toluene, n-hexane, acetone, dimenthylformamide, acetonitrile, dimethylsulfoxide, chloroform) were bought from Spectrochem Pvt. Ltd, India, dried and used for spectroscopic experimentation without further purification. N,N-Diethylaniline used for spectroscopic experiments was bought from Merck, India. It was redistilled, stored in dark and used under nitrogen atmosphere. Tetrahydrofuran, acetonitrile, acetone, chloroform and methanol used for synthesis were obtained from Fisher Scientific and used as received. Commercially available reagents viz. Nitrobenzyl bromide, 4-cyanobenzyl bromide, Triphenylphosphine and 9-anthracenecarboxaldehyde were purchased from Sigma-Aldrich, USA or Spectrochem Pvt. Ltd, India and used as received without any further purification. Sodium hydroxide and Potassium tertiary butoxide were bought from Avra Synthesis Pvt. Ltd and used as received. Detailed synthetic procedures and compound characterization are shown in the Supporting Information.

Photochemistry: UV-visible absorbance spectroscopy was performed in JASCO-V660 spectrophotometer at 298K. The fluorescence spectra were recorded in a Horiba Jobin Yvon Fluoromax-4 instrument at 298 K. For UV-visible experiments a two-faced transparent quartz cuvette of a path length of 1 cm was used and for fluorescence experiments a four-faced transparent quartz cuvette having path length 1 cm was used. The excitation and emission slit widths were kept equal in all cases. Time-resolved luminescence measurements were carried out in a Horiba Jobin Yvon Fluorocube instrument in a time-correlated single photon counting (TCSPC) arrangement. A 390 nm LED with a pulse repetition rate of 1 MHz was used as the light source for excitation of all the regiomers. The instrument response function (IRF) was collected using a scatterer (Ludox AS40, colloidal silica, Sigma-Aldrich). The detector response time (full-width at half-maxima) for both the LEDs was ~ 1 ns. The excited state decay has been collected fixing the

collection wavelength near the emission maxima of a given fluorophore. The excited state decay has been fitted using the IBH software DAS6 according to the equation:

$I(t)= \Sigma A_i iexp\ (-t/\tau_i)$

where, Ai = amplitude of the decay and τ_i is the corresponding lifetime.

All the UV-visible absorption, steady-state and time-resolved luminescence measurements were carried out fixing the concentration of fluorophores (*ortho-CN*, *meta-CN,* AnPh) at 40 μM. The concentration of N, N-DEA for the quenching studies was varied in the range of 0 M to 0.263 M.

Electrochemistry: Cyclic voltammetry (CV) measurements were carried out with PGSTAT204-Metrohm multi-Autolabpotentiostat/ galvanostat. A three-electrode setup having non-coated glassy carbon electrode (GCE) of 5 mm diameter was used as a working electrode. As a reference electrode Ag/Ag+ electrode and as a counter electrode, a platinum wire was used for all the electrochemical experiments. All the electrochemical studies were carried out in 0.1 M tetrabutylammoniumbromide (TBAB) as supporting electrolyte at 25°C. Acetonitrile solutions of the compounds (*ortho*-CN and *meta*-CN) were used for experimentation.

Femtosecond Transient Absorption Spectroscopy. The Transient absorption (TA) measurement was performed in a femtosecond pump probe set up (Helios Fire). A mode-locked Ti: sapphire oscillator (Vitara, coherent) was used to obtain the fundamental laser pulse center at 800 nm, having bandwidth (FWHM) 20 nm, pulse width 100 fs, 80 MHz repetition rate, and power of 400 nJ. A part of the fundamental laser beam was amplified using a regenerative amplifier (Astrella, coherent) to generate an amplified pulse with an energy of 6 mJ center at 800 nm having a pulse width of 35 fs, repetition rate 1 kHz, bandwidth 20 nm. Part of the amplified pulses was directed through an optical parametric amplifier (OPA) system to generate tunable pump pulses of interest.

Another part of the fundamental beam was focused on a 2 mm thick sapphire crystal to generate a white light continuum (WLC) probe. Then, pump (excitation) and probe (WLC) pulses were focused and overlapped on a 2 mm cuvette which contains the sample. Finally, after passing through the sample, the probe beam was collected using an optical fiber cable and a spectrometer embedded in the system (Helios Fire). The instrument response function (IRF) for the setup was determined to be about 110 fs. All measurements were carried out at 22°C temperature. All the samples were purged with nitrogen for 30 minutes before recording the TAS.

Nanosecond and femtosecond Transient Absorption Spectroscopy: The nano-second transient absorption spectra (ns-TAS) for all the samples were recorded using a nanosecond laser flash photolysis setup. The samples were photoexcited using the third harmonic of a Q-switched laser (Quanta Ray, Lab 150, Spectra Physics, USA) with pulse width ~ 8 ns. The transient signals were probed using a pulsed xenon lamp (150 W), a Czerny-Turner monochromator and a detector (Hamamatsu R-928 photomultiplier tube). The transient signals were captured using an Agilent Infinium digital storage oscilloscope. All measurements were carried out at 22°C temperature. All the samples were purged with nitrogen for 30 minutes before recording the TAS.

Computational Methods: Geometry optimization and molecular orbital (MO) energy level calculations for the two isomers were calculated using B3LYP/6-311(+)G(d,p) level of theory at PCM model in Gaussian 16 suite of program. Geometries of the radical anions were optimized using density functional theory (DFT) and time dependent density functional theory (TDDFT) with Spartan'18 (Wave function, 2018) using the B3LYP function. The basis sets 6-31G and 6-31G* were used for ground state and excited state optimization respectively. The (unpaired) spin density maps of the radical anions generated were obtained using the same program.

SI-B: Synthesis and Characterization of (E)-2-(2-(anthracen-9-yl) vinyl) benzonitrile (*ortho*-CN) and (E)-3-(2-(anthracen-9-yl) vinyl) benzonitrile (*meta*-CN)

In an oven dried round bottomed flask, *ortho*-cyanobenzyl bromide or *meta*-cyanobenzyl (1a, b) {1g, 5.1 mol} and triethylphosphite (4.4 ml, 5.1mmol) were taken together and refluxed overnight at 160 °C. The crude product was dried and used directly for the next step. Equimolar amount of this diethyl cyanobenzylphosphone (0.61 g, 2.42 mmol) and potassium tertiarybutoxide (0.27 g, 2.42 mmol) were added to 9-anthracenecarboxaldehyde (0.50g, 2.42 mmol) in dry THF (30 mL) and stirred at room temperature for 8 hours under nitrogen atmosphere to obtain yellow precipitate. The precipitate was purified in silica gel column using 33 % chloroform in hexane as eluent. Pure product was obtained as yellow solid (76%) and was characterized. The ^{1}H-NMR (Figure SI 1, 2) of *ortho*-CN and *meta*-CN isomer (3a, b) are provided below.

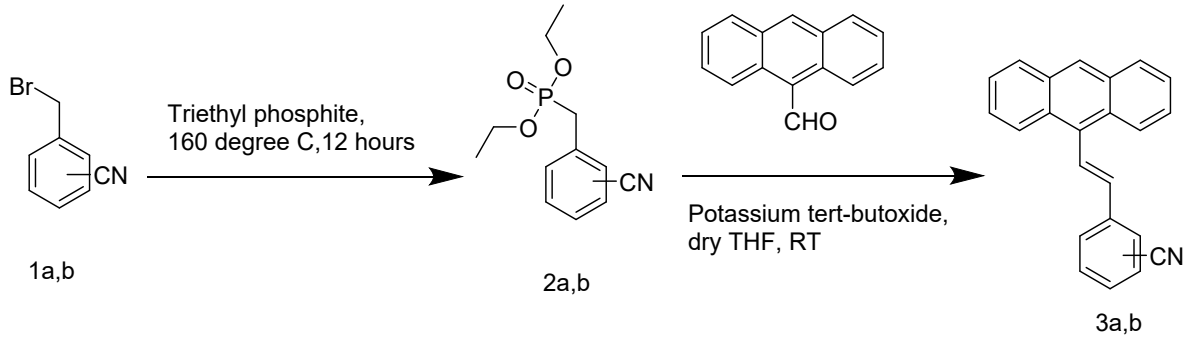

Scheme SI 1: Scheme of synthesis for the two isomeric compounds *ortho*-CN and *meta*-CN.

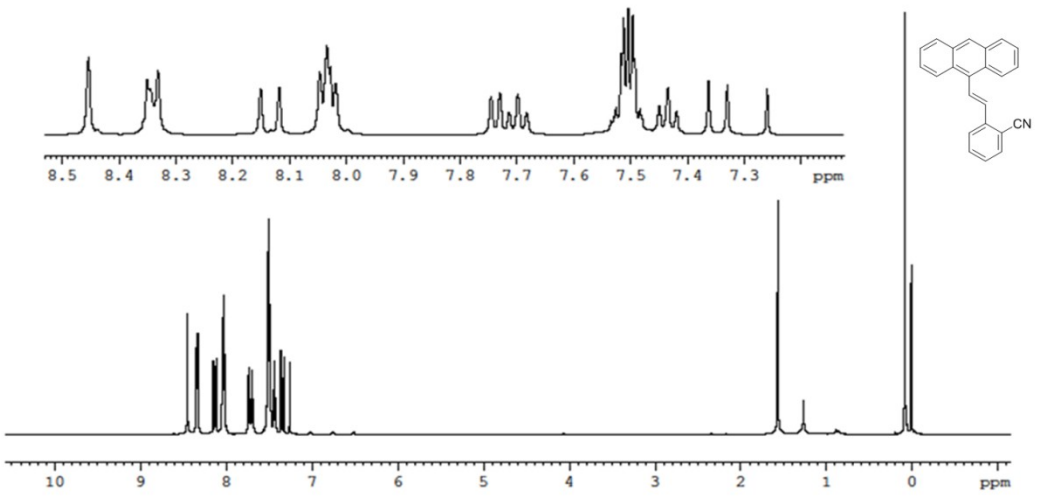

Figure S1: The proton NMR (^{1}H NMR) spectra of *ortho*-CN in $CDCl_3$: ^{1}H NMR ($CDCl_3$) δ: 7.35 (d, 1H, trans proton), 7.4-7.43 (m, 1H, anthracene), 7.4-7.5 (m, 4H, anthracene), 7.67-7.33(m, 2H, cyanobenzene 3,5 position), 7.98-8.03 (m, 3H, anthracene), 8.12 (d, 1H, trans proton), 8.25-8.30 (m, 2H, cyanobenzene 4,6 position), 8.4 (s, 1H, anthracene 10 position)

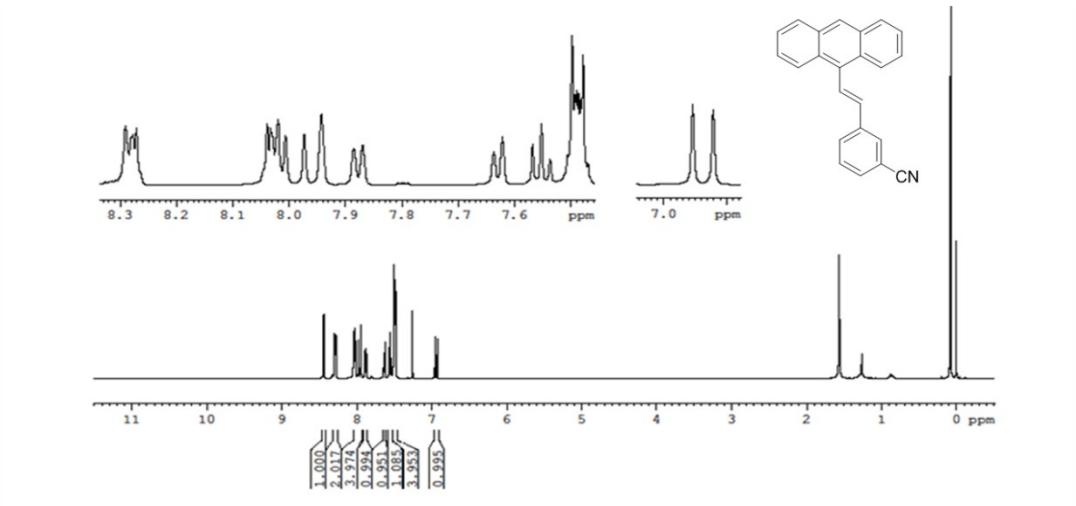

Figure S2: The proton NMR (^{1}H NMR) spectra of *meta*-CN in $CDCl_3$: ^{1}H NMR ($CDCl_3$) δ: 6.93 (d, 1H, trans proton), 7.46-7.67 (m, 4H, anthracene), 7.8-7.9 (m, 2H, anthracene), 7.95 (d, 1H, trans proton), 8.0 -8.06 (m, 4H, cyanobenzene), 8.27-8.28 (m, 2H, anthracene), 8.43 (s, 1H, anthracene 10 position)

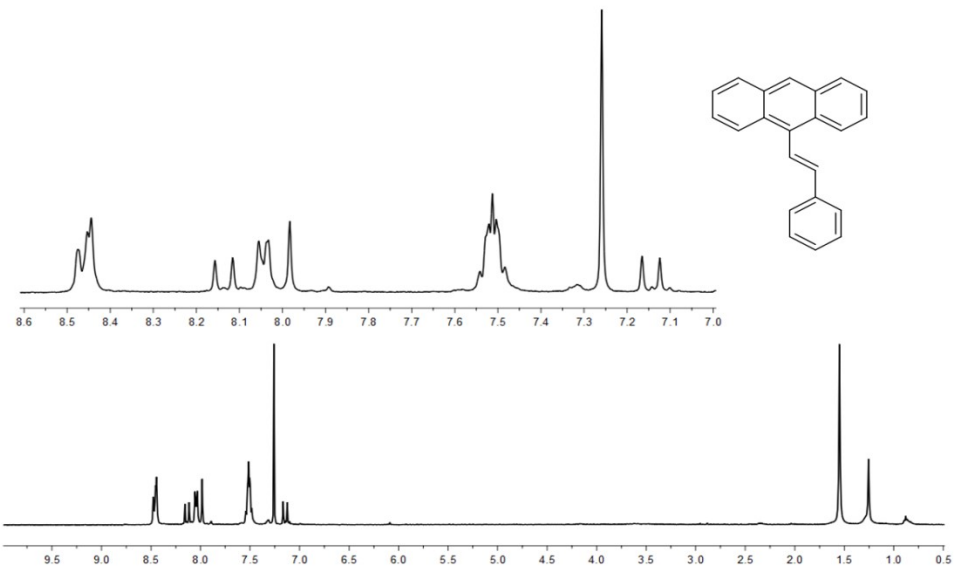

Figure S3: The proton NMR (^{1}H NMR) spectra of AnPh in $CDCl_3$: ^{1}H NMR ($CDCl_3$) δ: 7.15 (d, 1H, Trans proton), 7.48-7.54 (m, 4H, anthracene), 7.45-7.6 (m, 2H, anthracene), 7.94 -8.03(s, 1H, anthracene 10 position), 8.15 (d, 1H, Trans proton), 8.27-8.28 (m, 2H, anthracene), 8.43 (m, 5H)

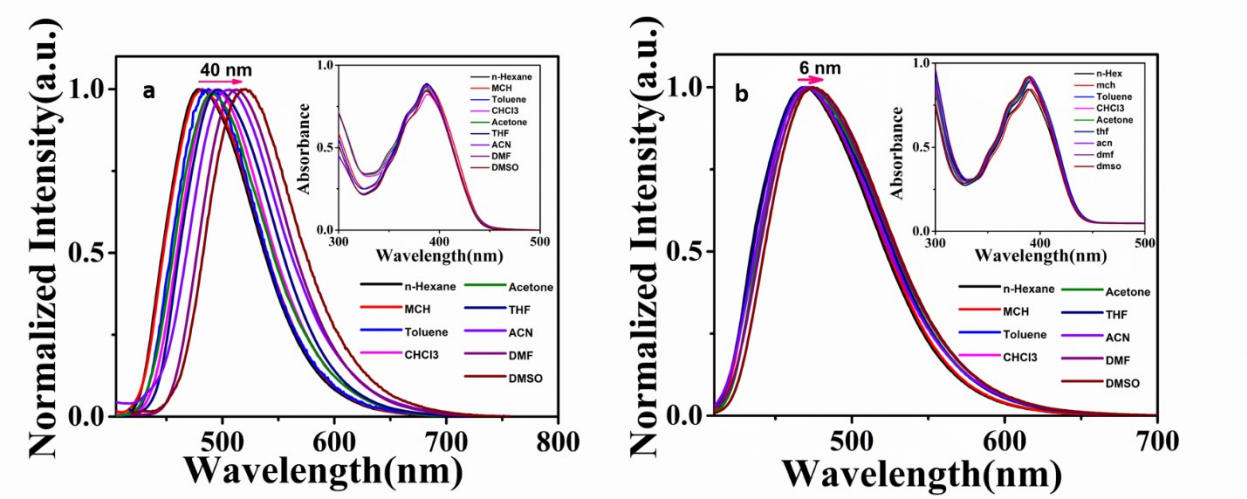

Figure S4: Normalized steady state luminescence spectra of (a) *ortho*-CN and (b) *meta*-CN in different polarity solvents (Inset: UV-vis absorption spectra of the isomers in different solvents) (λex = 390 nm, [*ortho*-CN] =[*meta*-CN] =40 µM)

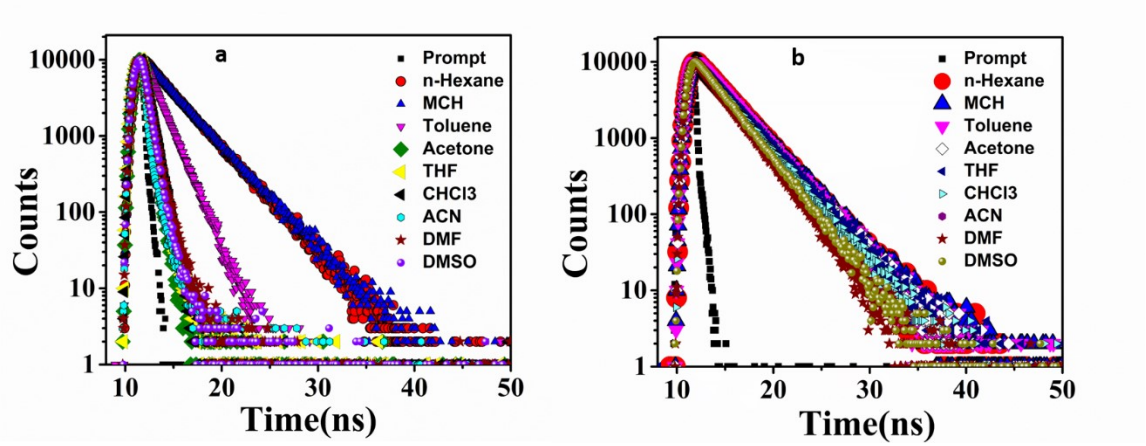

Figure S5: Time resolved luminescence spectra of (a) *ortho*-CN and (b) *meta*-CN in different polarity solvents (λex = 390 nm, λcoll = 500 nm, [*ortho*-CN] =[*meta*-CN] =40 µM)

Table S1: Luminescence lifetime values *ortho*-CN and *meta*-CN in varying polarity solvent (λex = 390 nm, λcoll = 500 nm). The life time values have 1-2% error bar.

Isomer	***ortho*-CN**			***meta*-CN**		
Solvents	**τ_1, B1 (%)**	**τ_2, B1 (%)**	**χ^2**	**τ_1, B1 (%)**	**τ_2, B1 (%)**	**χ^2**
n-Hexane	3.01 ns,100	-	1.01	3.05 ns, 100	-	0.99
MCH	3.05 ns, 100	-	1.12	3.16 ns, 100	-	1.05
Toluene	1.45 ns, 89.61	0.63ns, 10.39	1.01	3.17 ns, 100	-	1.05
Acetone	0.40 ns, 93.60	3.2 ns, 6.40	0.99	3.03 ns, 100	-	0.99
CHCl3	0.53 ns, 97.01	2.9ns, 2.99	1.04	2.95 ns ,100	-	1.1
THF	0.57 ns, 98.42	3.5 ns,1.58	1.06	3.10 ns, 100	-	1.09
ACN	0.41 ns, 91.43	0.95 ns, 8.57	1.1	2.94 ns, 100	-	0.99
DMF	0.34 ns ,70.35	0.88 ns, 29.65	1.03	2.57ns, 100	-	1.01
DMSO	0.38 ns, 76.56	0.78 ns, 23.44	0.99	2.69 ns, 100	-	1.07

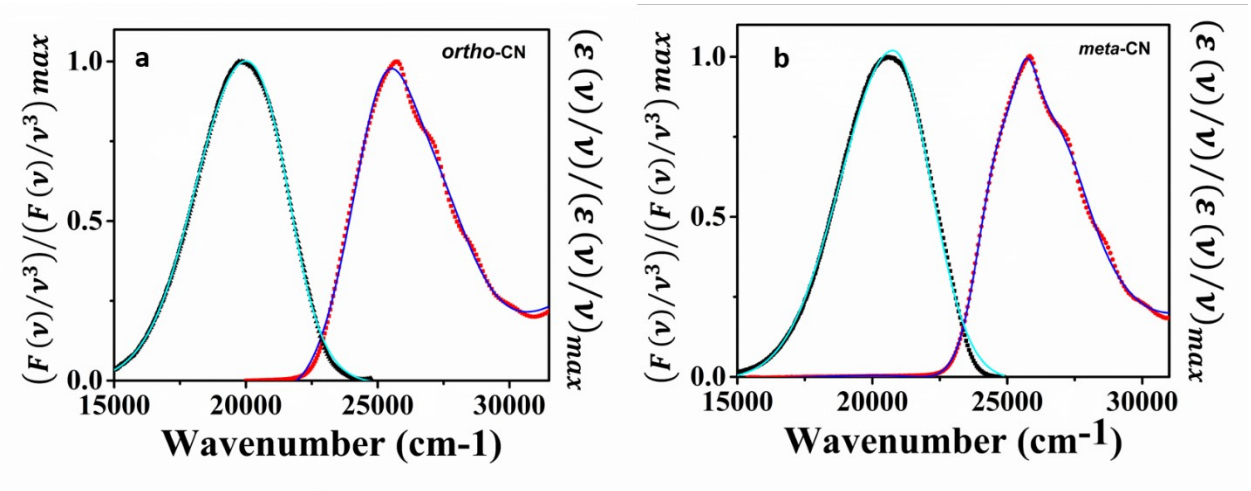

Figure S6: Steady state emission and absorption spectra of (a) *ortho*-CN and (b) *meta*-CN isomer in MCH. The experimental spectra (dotted points) are fitted to Einstein B coefficient absorption and emission line shapes (solid lines). ([*ortho*-CN] =[*meta*-CN] =40 µM).

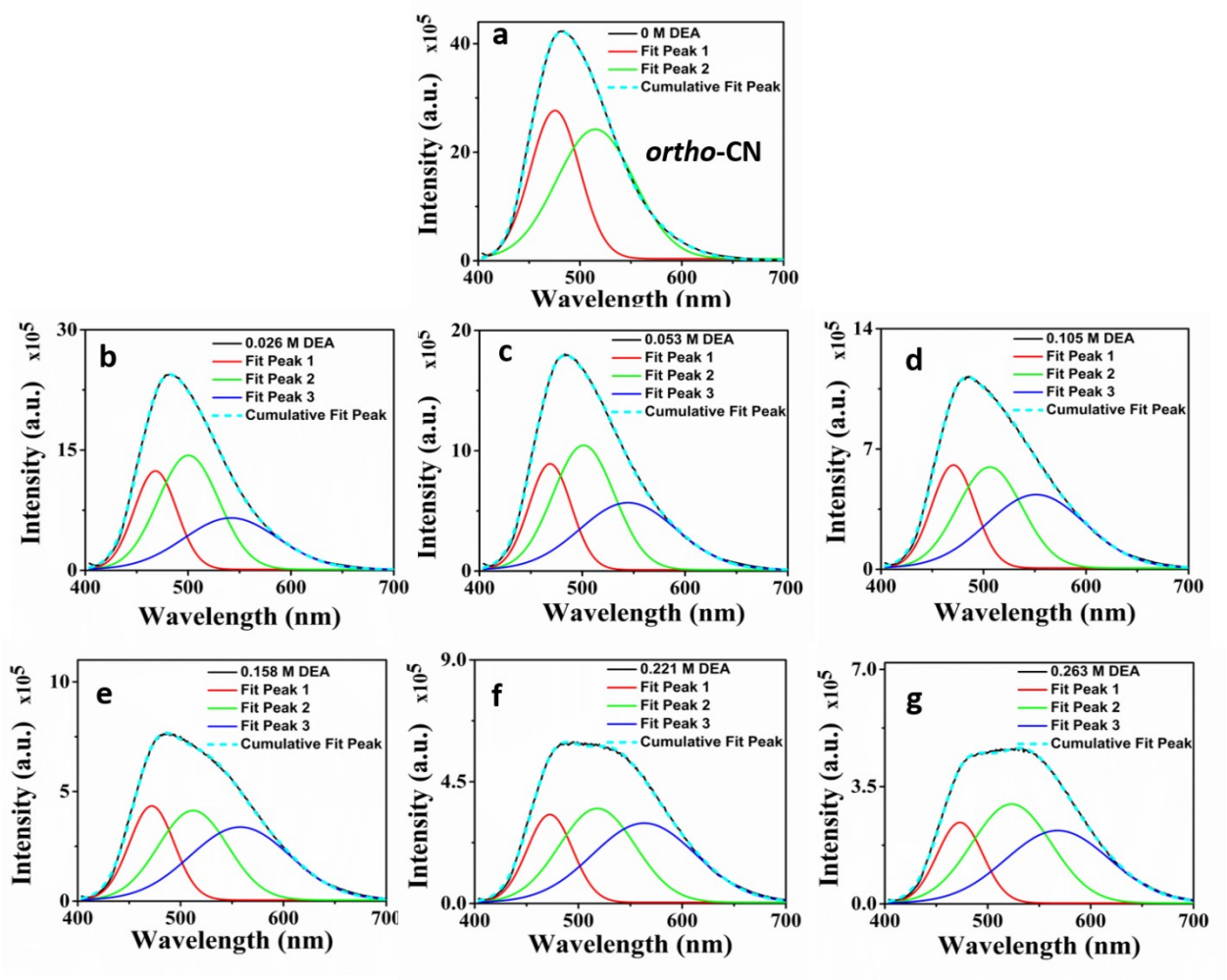

Figure S7: Deconvolution of emission spectra of ortho-CN (a) in absence and (b-g) in presence of increasing concentration of DEA in MCH using Gaussian curves fitting technique (λex = 390 nm, [*ortho*-CN] =40 µM). Band 1 and 2 are vibrionic progression of the LE emission of ortho-CN and band 3 is the exciplex emission.

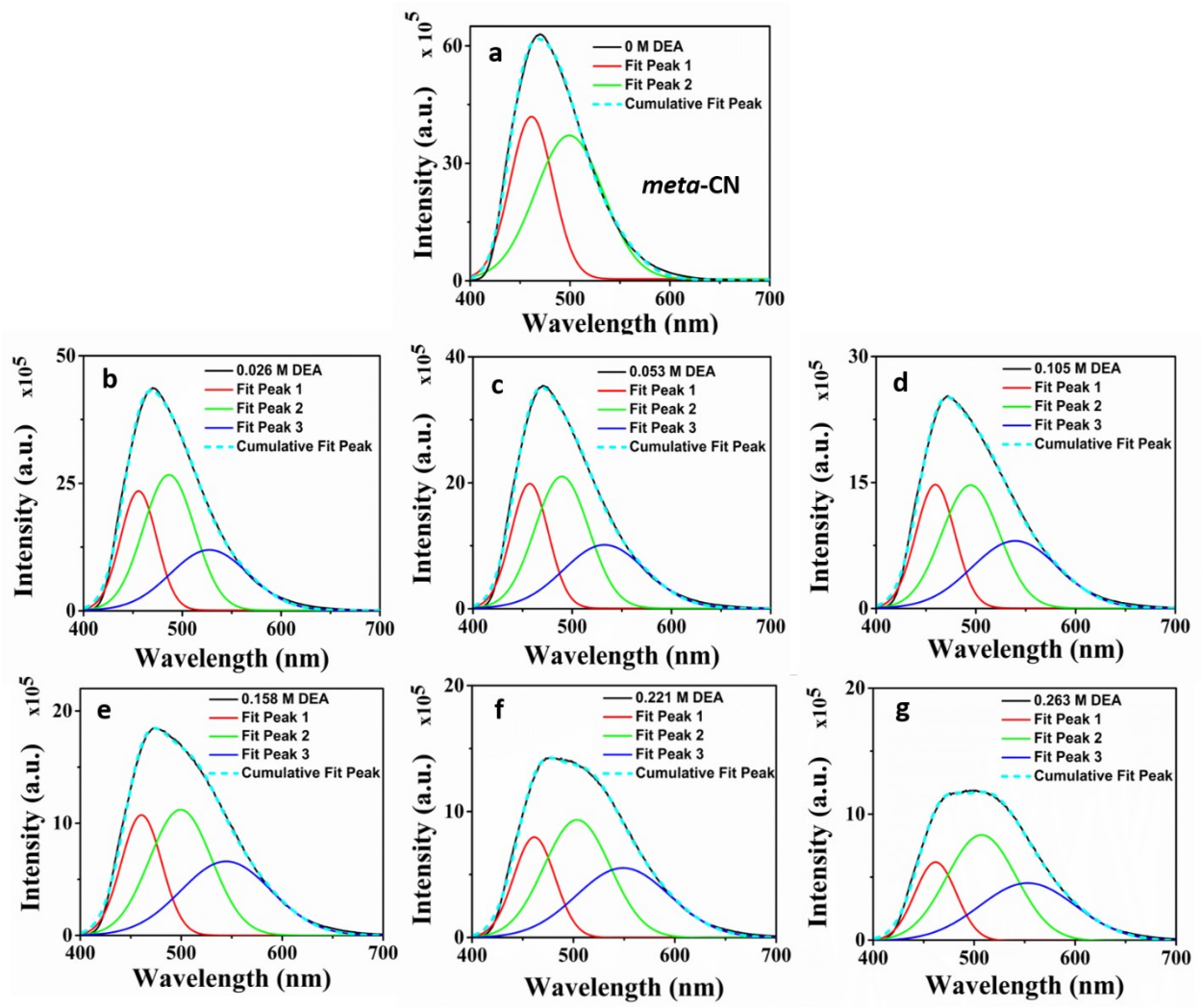

Figure S8: Deconvolution of emission spectra of *meta*-CN (a) in absence and (b-g) in presence of increasing concentration of DEA in MCH using Gaussian curves fitting technique (λex = 390 nm, [*meta*-CN] =40 µM). Band 1 and 2 are vibrionic progression of the LE emission of *meta*-CN and band 3 is emission upon exciplex formation upon DEA addition.

Table S2: Luminescence lifetime values of *ortho*-CN and *meta*-CN in MCH in presence of various concentrations of DEA (0–0.263 M), (λ_{ex} = 390 nm, λ_{coll} = 500 nm). The life time values have 1-2% error bar.

Isomer	***ortho*-CN**			***meta*-CN**		
[DEA] (M)	**τ_1, B_1 (%)**	**τ_2, B_2 (%)**	**χ^2**	**τ_1, B_1 (%)**	**τ_2, B_1 (%)**	**χ^2**
0	3.05 ns, 100	-	1.24	3.16 ns, 100	-	1.05
0.026	1.61 ns,91.04	10.5 9 ns, 8.96	1.16	1.81 ns, 72.08	9.8 ns, 27.92	1.09
0.053	1.22 ns, 90	10.68 ns, 10	1.24	1.30 ns, 62.11	10.45 ns, 37.89	1.07
0.105	0.79 ns, 87.55	11.68 ns, 12.45	1.26	0.86 ns, 52.78	11.12 ns, 47.22	1.09
0.158	0.58 ns, 84.86	11.80 ns, 15.14	1.05	0.64 ns, 48.41	11.3 ns, 51.59	0.99
0.211	0.43 ns, 82.31	11.98 ns, 17.69	1.01	0.52 ns, 43.86	11.58 ns, 56.14	1.05
0.263	0.36 ns, 49.03	12.56 ns, 50.97	1.03	0.43 ns, 39.70	11.75 ns, 60.30	1.03

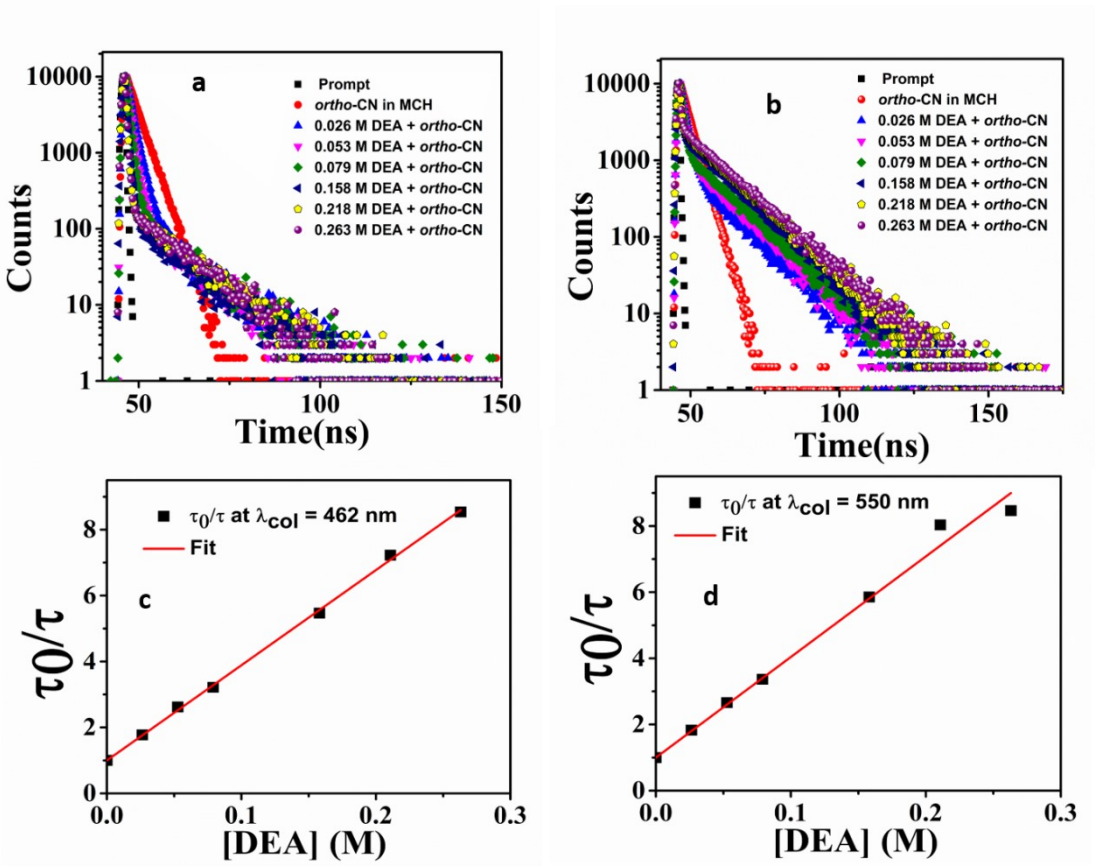

Figure S9: Time-resolved luminescence quenching studies of *ortho*-CN isomer in MCH with increasing concentration of DEA [0 M–0.263 M] for emission wavelength (λcoll) of (a) 462 nm and (b) 550 nm. SV plot of time resolved luminescence quenching of *ortho*-CN for emission wavelength (λcoll) of (c) 462 nm and (d) 550 nm.

Table S3: Luminescence lifetime values of *ortho*-CN in MCH in presence of various concentrations of DEA (0–0.263 M) at monomer emission (λcoll = 462 nm) and excimer emission wavelength (λcoll =550 nm). The life time values have 1-2% error bar. λex = 390 nm

***ortho*-CN**	**λcoll = 462 nm**			**λcoll = 550 nm**		
[DEA] (M)	**τ_1, B_1 (%)**	**τ_2, B_2 (%)**	**χ^2**	**τ_1, B_1 (%)**	**τ_2, B_1 (%)**	**χ^2**
0	3.15 ns, 100	-	1.24	3.05 ns, 100	-	1.05
0.026	1.76 ns,93.39	10.68 ns, 6.61	1.16	1.71 ns, 73.43	11.80 ns, 26.57	1.09
0.053	1.19 ns, 92.30	11.26ns, 7.70	1.24	1.78 ns, 60.06	11.89 ns, 39.94	1.07
0.079	0.97 ns, 90.67	11.47 ns, 9.33	1.26	0.86 ns, 52.63	12.04 ns, 47.37	1.09
0.158	0.57 ns, 92.09	11.34 ns, 7.91	1.05	0.64 ns, 38.71	12.19 ns, 61.29	0.99
0.211	0.43 ns, 90.88	11.57 ns, 9.12	1.01	0.52 ns, 33.70	12.37 ns, 66.30	1.05
0.263	0.37 ns, 89.82	11.94 ns, 10.18	1.03	0.43 ns, 30.83	12.39 ns, 69.17	1.03

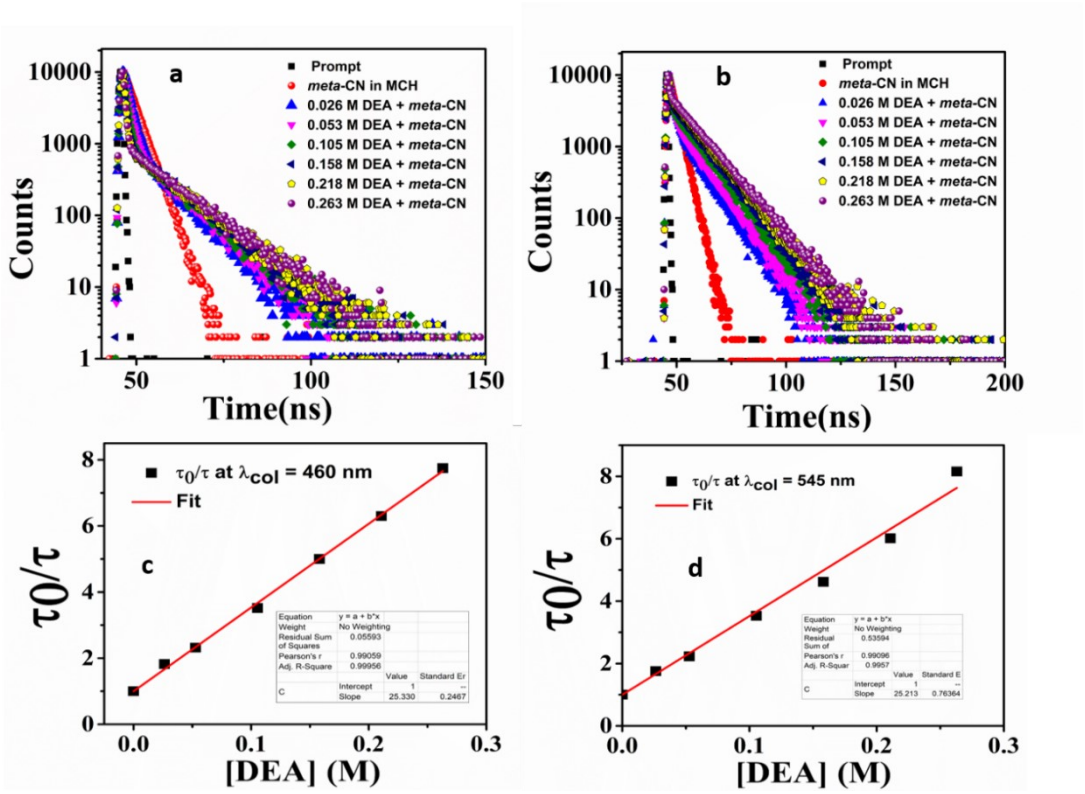

Figure S10: Time-resolved luminescence quenching studies of *meta*-CN isomer in MCH with increasing concentration of DEA [0 M–0.263 M] for emission wavelength (λcoll) of (a) 460 nm and (b) 545 nm. SV plot of time resolved luminescence quenching of *meta*-CN for emission wavelength (λcoll) of (c) 460 nm and (d) 545 nm.

Table S4: Luminescence lifetime values of *meta*-CN in MCH in presence of various concentrations of DEA (0–0.263 M) at monomer emission (λcoll = 460 nm) and excimer emission wavelength (λcoll = 545 nm). The life time values have 1-2% error bar. λex = 390 nm

***meta*-CN**	**λcoll = 460 nm**			**λcoll = 545 nm**		
[DEA] (M)	**τ_1, B_1 (%)**	**τ_2, B_2 (%)**	**χ^2**	**τ_1, B_1 (%)**	**τ_2, B_1 (%)**	**χ^2**
0	3.15 ns, 100	-	1.04	3.13 ns, 100	-	1.05
0.026	1.72 ns,73.54	9.30 ns, 26.46	0.99	1.79 ns, 51.01	9.69 ns, 48.99	1.07
0.053	1.35 ns, 70.20	10.08 ns, 29.80	1.04	1.42 ns, 41.02	10.40 ns, 58.98	1.02
0.105	0.89 ns, 64.30	10.82 ns, 35.70	0.99	0.90 ns, 25.97	11.10 ns, 74.09	1.01
0.158	0.62 ns, 62.26	11.10 ns, 37.74	1.07	0.68 ns, 20.13	11.31 ns, 79.87	1.02
0.211	0.49 ns, 61.77	11.7 ns, 38.23	1.00	0.52 ns, 17.27	11.77 ns, 82.73	1.01
0.263	0.41 ns, 60.60	11.85 ns, 30.40	1.03	0.38 ns, 15.31	12.01 ns, 84.69	0.99

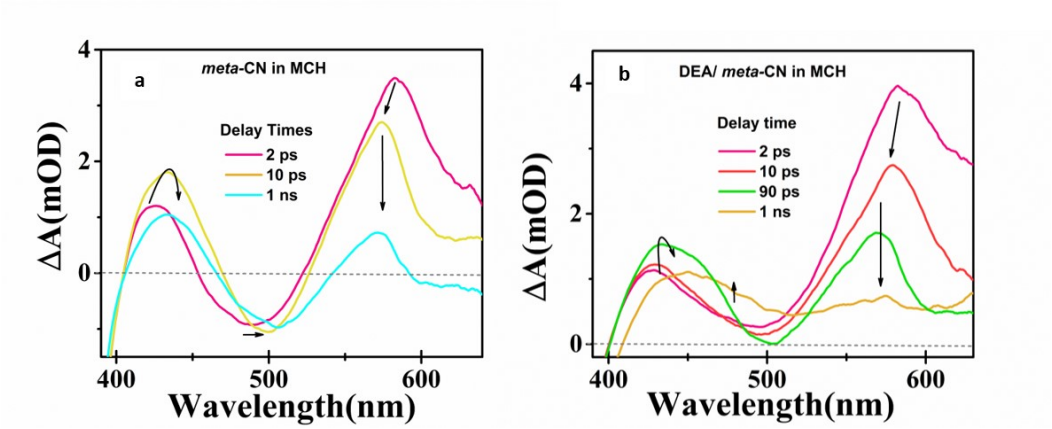

Figure S11: **Fs-Transient absorption spectra of *meta*-CN in absence (a) and in presence (b) of DEA. (λex at 350nm, [DEA]=0.263 M, [*meta*-CN] = 40 µM)**

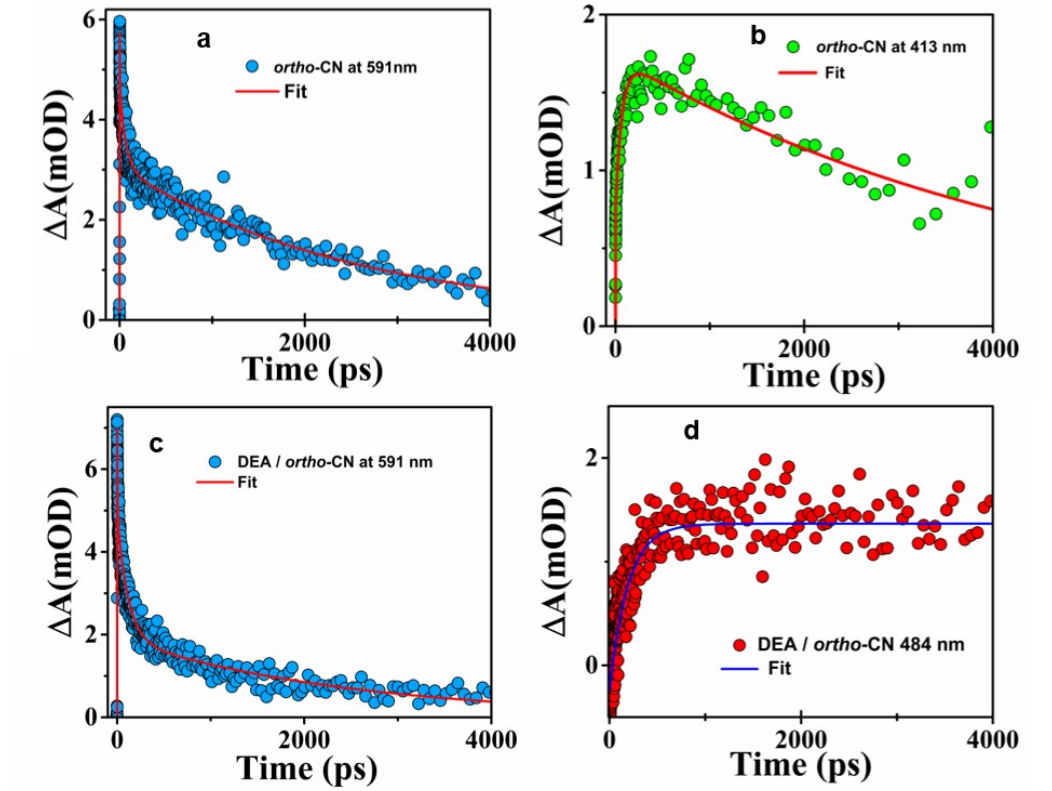

Figure S12: **Kinetic traces derived from the fs-TA spectra of *ortho*-CN isomer in MCH at (a) 591 nm and (b) 413 nm and DEA/*ortho*-CN in MCH at (c) 591 nm (d) 484nm. (λex at 350 nm, [DEA]=0.263 µM, [*ortho*-CN] = 40 µM)**

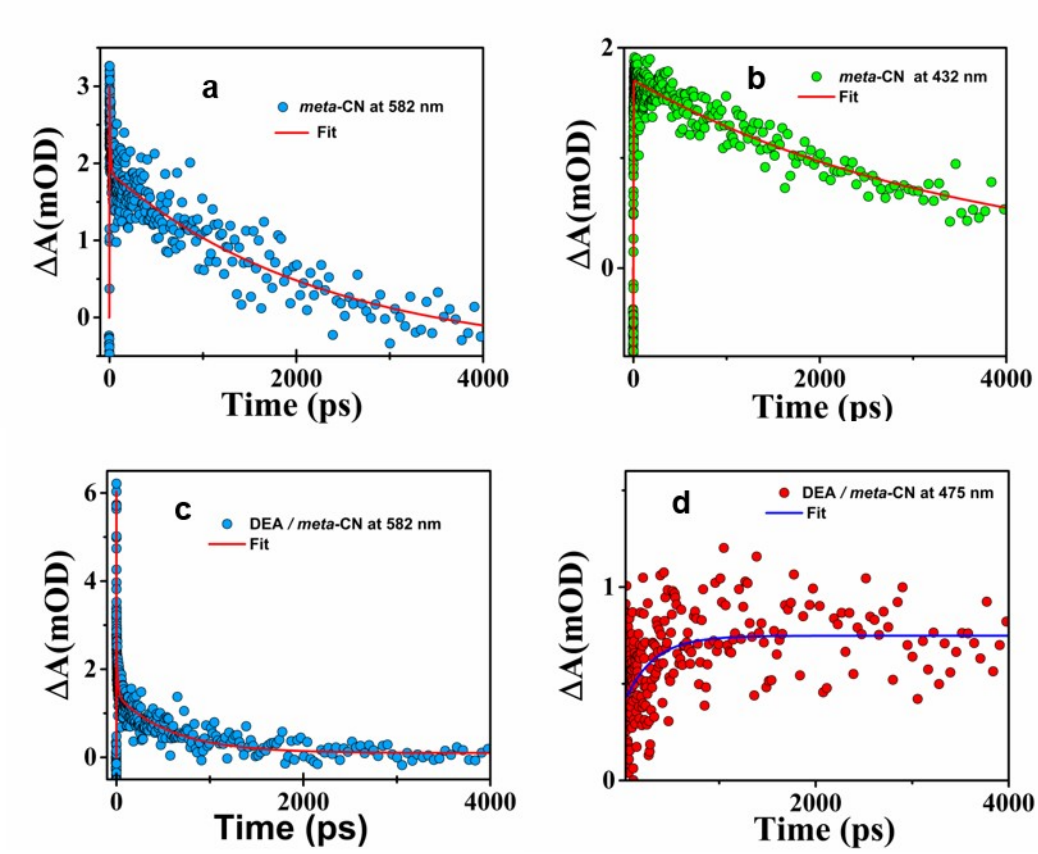

Figure S13: **Kinetic traces derived from the fs-TA spectra of *meta*-CN isomer in MCH at (a) 582 nm and (b) 432 nm and DEA/*meta*-CN in MCH at (c) 582 nm and (d) 475 nm. (λex at 350 nm, [DEA]=0.263 µM, [*meta*-CN] = 40 µM)**

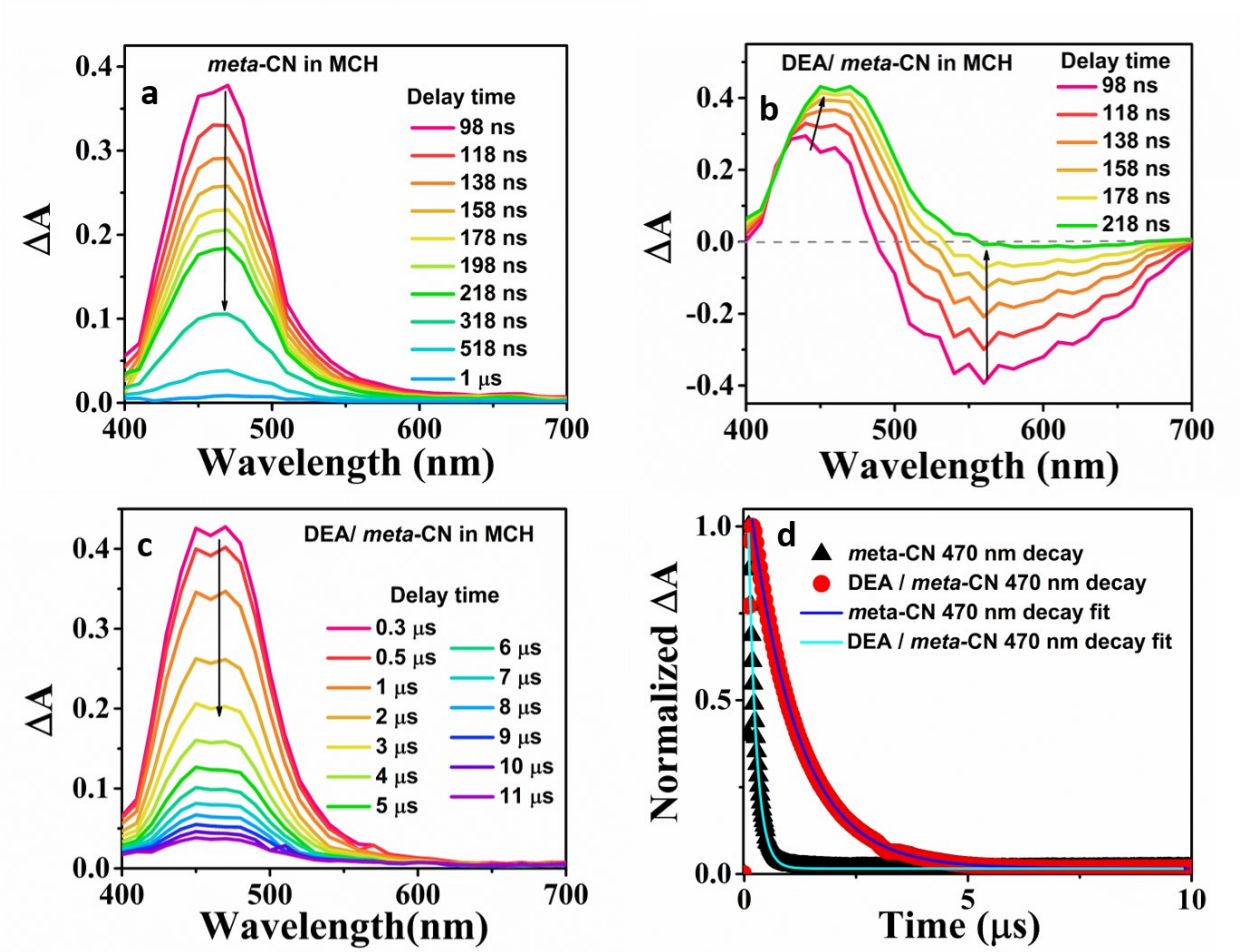

Figure S14: **Nanosecond transient absorption spectra of *meta-CN* (40 μM) in MCH (a) in absence of any quencher and (b, c) in presence of DEA (0.263 M). (d) Comparative decay trace of *meta-CN* isomer in absence and presence of electron donor at 470 nm; spectra were recorded in MCH after pulsed excitation at 355 nm under N_2 at 22°C.**

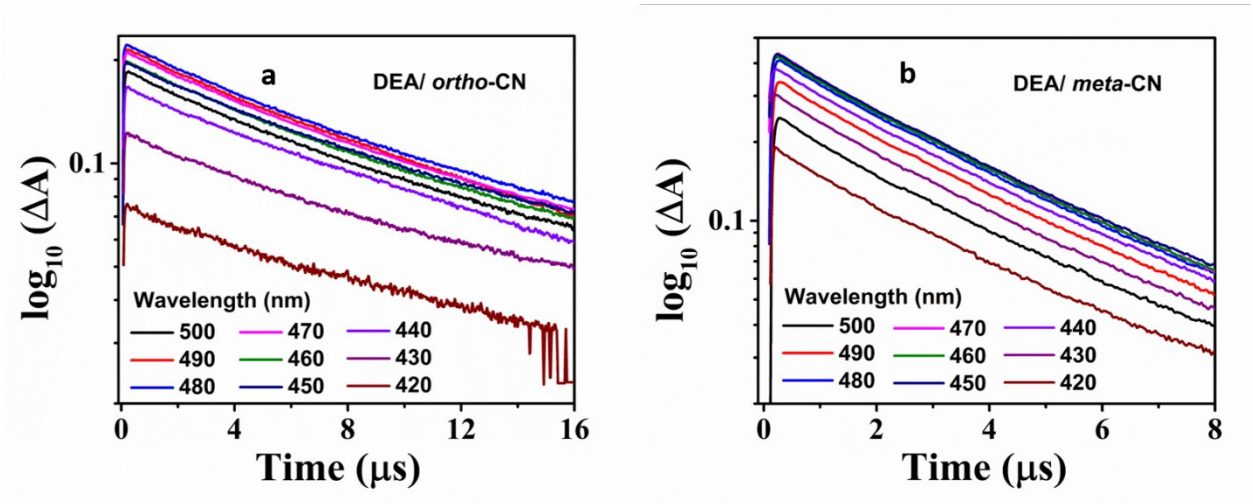

Figure S15: Semi-logarithmic plot of ns transient absorption data of (a) DEA/ *ortho*-CN and (b)DEA/ *meta*-CN in MCH at wavelength range of 420 nm - 500 nm. The decays are observed to be single-exponential for DEA/ ortho-CN as well as for DEA/meta-CN.

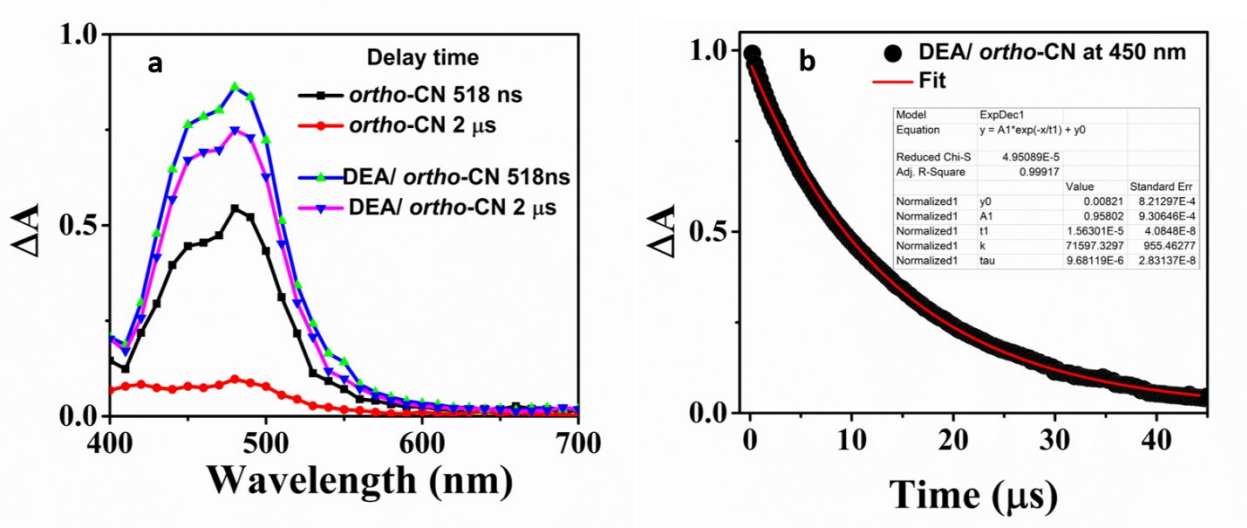

Figure S16: (a) Compared nanosecond transient absorption spectra of *ortho*-CN in absence and in presence of DEA at same delay times (518 ns and 2 μs). (b) Decay trace of DEA/ *ortho*-CN at 450 nm in MCH.

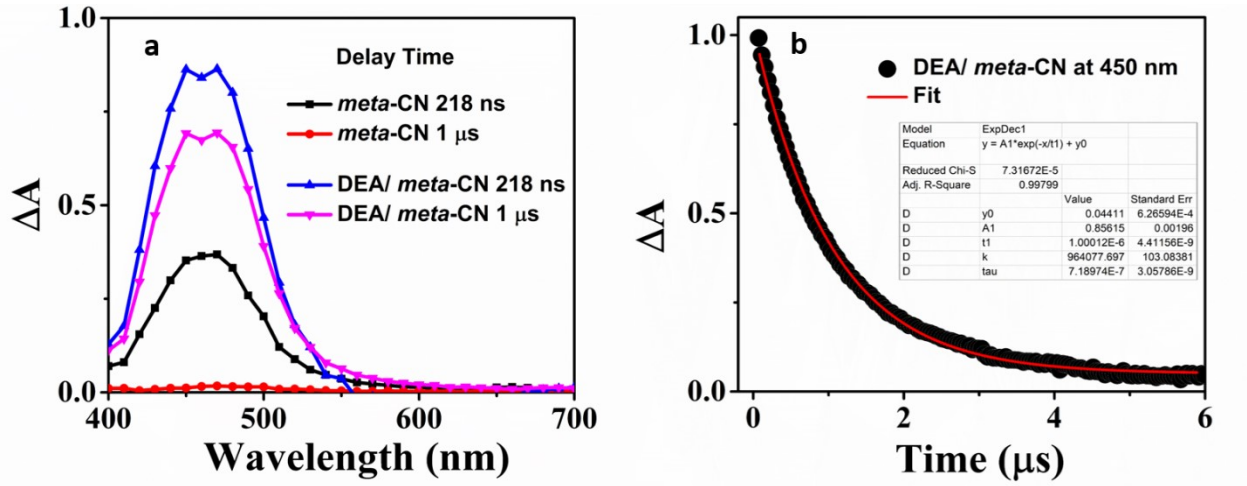

Figure S17: (a) Compared nanosecond transient absorption spectra of *meta*-CN in absence and in presence of DEA at same delay times (218 ns and 1 μs). (b) Decay trace of DEA/ *meta*-CN at 450 nm in MCH.

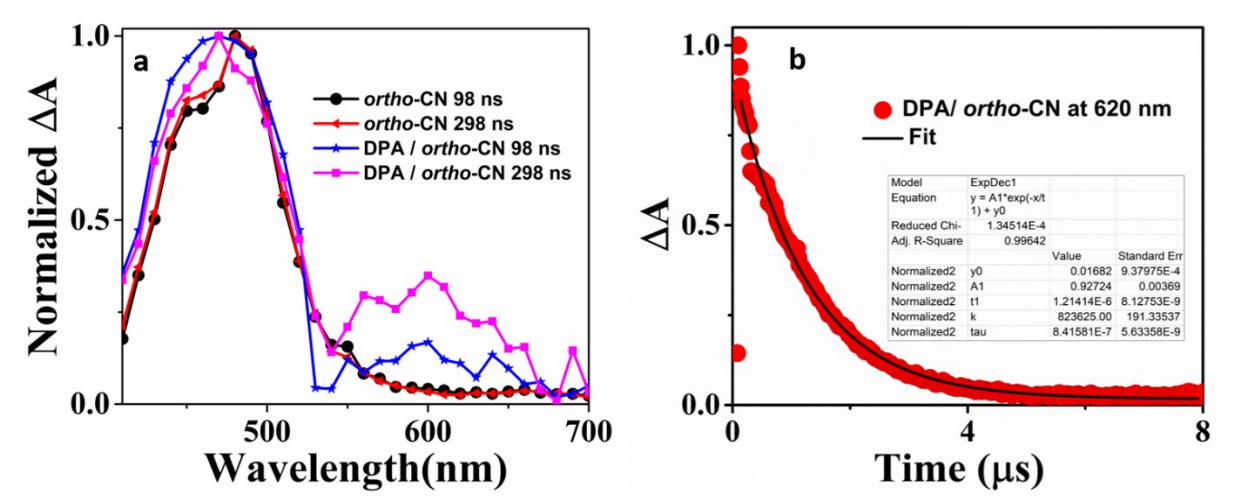

Figure S18: TAS spectra of *ortho*-CN and DPA/ *ortho*-CN plotted together at two different time delays (λ_{ex} = 355 nm). The spectrum clearly reveals formation of the broad band at ~620 nm due to the diphenylamine radical cation upon the addition of the DPA.

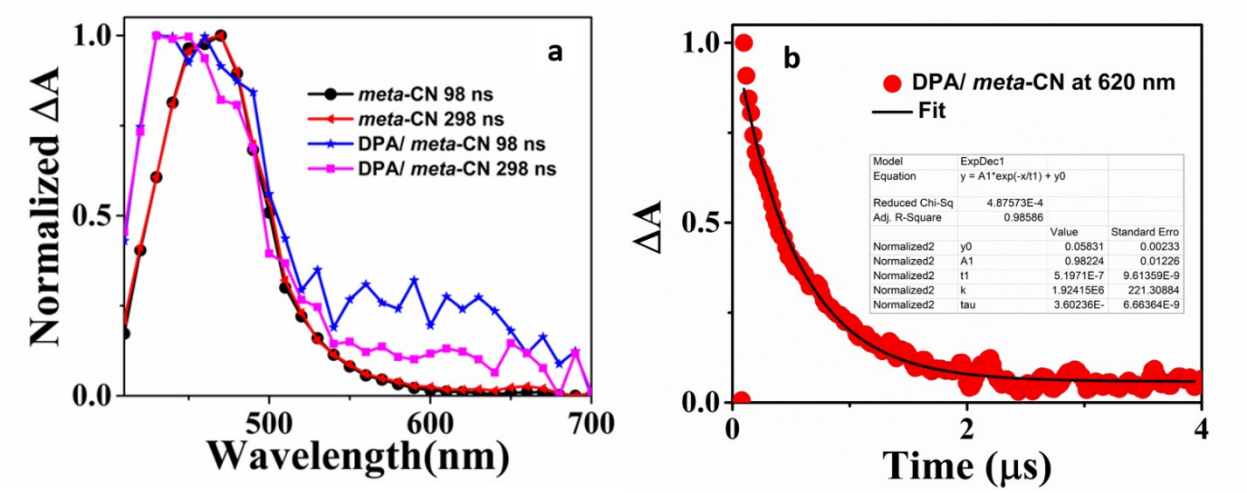

Figure S19: TAS spectra of *meta*-CN and DPA/ *meta*-CN plotted together at two different time delays. The spectrum clearly reveals formation of the broad band at ~620 nm due to the diphenylamine radical cation upon the addition of the diphenylamine.

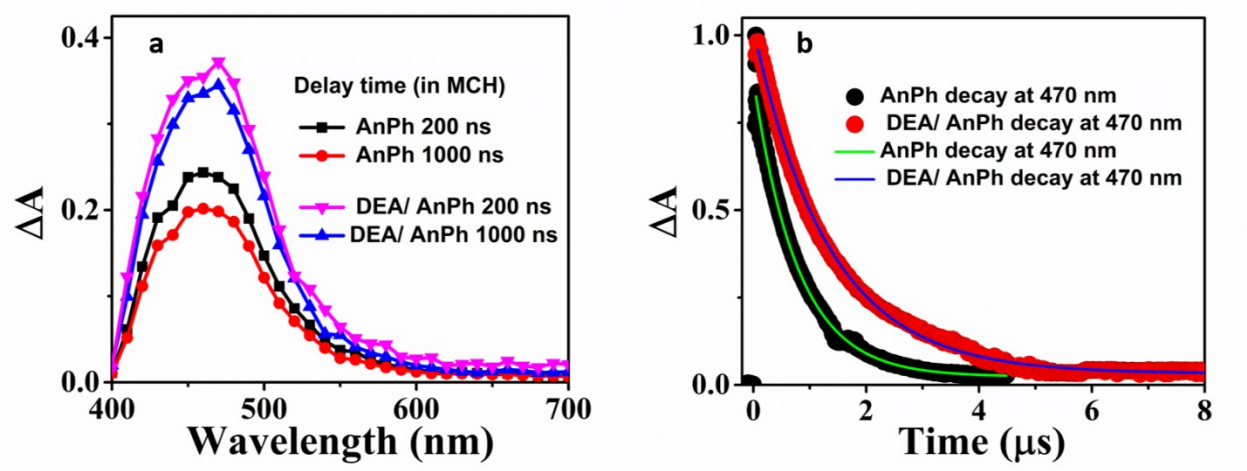

Figure S20: (a) ns-TAS spectra of AnPh (40 μM) and DEA/AnPh (0.263 M) in MCH plotted together at two different time delays of 500 ns and 1000 ns (λex = 355 nm). (b) Normalized decay trace of AnPh in absence and presence of electron donor at 470 nm. The spectrum clearly reveals the positive absorption band at around 460 nm at same delay times is much more intense in presence of DEA than that of free AnPh. The transient traces for the excited-state band exhibits a faster decay time component for the free AnPh compared to that for the DEA/AnPh associations.